

# Development of a New Inertial-based Vibration Absorber for the Active Vibration Control of Flexible Structures

Carmine Maria Pappalardo, Domenico Guida

**Abstract**—In this paper, a new actively controlled inertial-based vibration absorber is proposed and used for controlling the mechanical deformations of flexible structures. To this end, a method for reducing the externally induced vibrations of structural systems is developed. The method employed in this paper is based on the numerical techniques of the applied system identification field and is grounded in the optimal control theory. A three-story shear building system with a pendulum hinged on the third floor is the flexible structure considered as the case study of this investigation. This mechanical system is constructed using rigid and flexible components in order to reproduce a simple three-dimensional structure. The base of the structural system is excited by a harmonic excitation combined with a noise excitation source in order to simulate the earthquake. By doing so, the worst case scenario in which the frequencies of the external excitation are close to the natural frequencies of the flexible structure is considered. The pendulum mounted on the third floor of the flexible structure serves as an actively controlled inertial-based vibration absorber. The control torque applied to the pendulum is actively controlled by using a brushless motor driven by a programmable digital controller. Therefore, the inertial effects of the oscillating pendulum directly contrast the externally induced vibrations of the three-story shear building system. The feedback control torque applied on the pendulum is obtained by monitoring the accelerations of the three floors of the flexible structure and is designed employing a realistic mechanical model of the dynamical system obtained by using a time-domain system identification approach. The numerical results found in this investigation by using a simple computer program coded in MATLAB show that the modal parameters identified for describing the dynamic behavior of the flexible structure are consistent with those predicted employing a simple lumped parameter model. Furthermore, in this investigation, an optimal closed-loop controller based on the Linear-Quadratic Regulator (LQR) method and an optimal state observer based on the Kalman filtering approach, also known as Linear-Quadratic Estimator (LQE), are designed employing the state-space model obtained from experimental data. Experimental results demonstrate that a considerable reduction of the structural vibrations of the three-story shear building system can be obtained by means of the introduction of the feedback controller combined with the state estimator.

**Index Terms**—Three-story shear building system, System identification, Optimal control, State estimation, Experimental modal parameter identification.

## I. INTRODUCTION

This paper is focused on the design and implementation of a new inertial-based vibration absorber for the active

C. M. Pappalardo is with the *Department of Industrial Engineering, University of Salerno*, Via Giovanni Paolo II, 132, 84084 Fisciano, Salerno, ITALY (corresponding author, email: cpappalardo@unisa.it).

D. Guida is with the *Department of Industrial Engineering, University of Salerno*, Via Giovanni Paolo II, 132, 84084 Fisciano, Salerno, ITALY (email: guida@unisa.it).

vibration control of flexible structures. For this purpose, an optimal controller is developed for reducing the mechanical vibrations of structural systems considering the applied system identification computational techniques. In this section, background material, the formulation of the problem of interest for this study, the scope and the contribution of this investigation, and the organization of the manuscript are provided.

### A. Background Material

Applied system identification can be seen as the complex process of developing mathematical models of dynamical systems based on input-output data [1]–[3]. In general, a mathematical model of a physical system can be used to predict by means of numerical simulations the system dynamic behavior in response to known external excitations [4]–[8]. In the field of applied system identification, the basic laws of mechanics are combined with statistical methods in order to devise mathematical models of dynamical systems by using experimental measurements. Model reduction techniques and the methodologies for the optimal design of experiments are also widely employed in the field of applied system identification [9]–[12]. In this context, numerical experiments obtained by means of dynamic simulations can be performed by using a reliable mathematical model of a physical system in order to reproduce the input-output relationships observed experimentally [13]–[17].

In the field of mechanical engineering, the consistent formulation of the equations of motion that describe the nonlinear behavior of a mechanical system represents a fundamental step in the solution of the optimal control, estimation, and identification problems [18], [19]. In this respect, the main challenge is represented by the fact that, in general, the linearized version of the equations of motion is inadequate for capturing the fully nonlinear physics of the problem at hand and, therefore, more advanced control algorithms, estimation techniques, and design methods are necessary for solving these difficult tasks [20], [21]. On the other hand, in several practical applications, using the fully nonlinear dynamic equations for predicting the time evolution of a mechanical system and calculating the control actions for the mechanical system employing the numerical solutions of the nonlinear set of dynamic equations can be difficult, if not impossible, to achieve or implement in real time [22]. One direction of research devoted to the solution of these important issues is based on the direct application of complex control strategies to a simplified, but still nonlinear, version of the equations of motion of the

mechanical system of interest [23]. To this end, one can use the optimal control theory based on the Pontryagin minimum principle leading to the Hamilton-Jacobi-Bellman partial differential equation, that is the continuous-time analogue of the discrete deterministic dynamic programming algorithm, or to a set of nonlinear differential-algebraic equations which form a nonlinear two-point boundary value problem which can be numerical solved by using the adjoint approach. Moreover, one can also use other effective analytical and computational methods for the design of nonlinear control actions. For instance, the feedback linearization approach, the nonlinear H-infinity control method, the sliding mode control algorithm, the nonlinear control strategies based on the control-Lyapunov function, and the extended Kalman filter approach represent, among the others, valid computational algorithms which can be effectively employed for the construction of a nonlinear control and estimation scheme [24]–[27]. However, as discussed in details in this paper, the linear control method of interest for this investigation is based on the optimal control and estimation approach since, in the case of small deformations, the structural system of interest can be adequately modeled as a linear dynamical system.

#### *B. Formulation of the Problem of Interest for this Study*

In the fields of dynamic and control engineering, applied system identification deals with the development of mechanical models of physical systems necessary for the design of open-loop (feedforward) and closed-loop (feedback) control strategies by using experimental measurements [28]–[32]. Thus, several investigations based on system identification techniques focused on the design of effective control strategies for machines and structures can be found in the literature [33]–[37]. However, all the identification analytical methods and numerical procedures employed in this important field of research have in common some fundamental principles and mathematical tools [38], [39]. In particular, the time-domain numerical procedures of applied system investigation are of interest for this investigation because the first-order dynamic models based on the state-space representation and the second-order dynamic models based on the configuration-space representation can be readily used for developing optimal controller and observer systems by using effective and robust control algorithms such as, for example, the Linear Quadratic Gaussian (LQG) regulation method [40]–[44]. For instance, important practical applications of the system identification methodologies are the refinement of finite element models of aerospace systems by using dynamic testing, the modal parameters identification of civil structures based on environmental and artificial vibrations, and the real-time identification of mechanical models of suspension mechanisms for implementing the active and semi-active control paradigms [45]–[53]. Furthermore, the nonlinear control methods based on the techniques of applied system identification are also useful for determining structural parameters of mechanical systems composed of rigid and flexible bodies connected by kinematic constraints that are referred to as multibody systems [54]–[59].

#### *C. Scope and Contributions of this Investigation*

This paper deals with the development of a control system capable of reducing the vibration of flexible structures based on a methodology for identifying first-order and second-order dynamic models of mechanical systems using time-domain input-output measurements. The proposed approach relies on the optimal control theory, is based on the numerical techniques of applied system identification, and is verified experimentally by using a simple test rig. The flexible structure considered for testing the proposed method is a three-story shear building system. A pendulum is hinged on the third floor of the flexible structure in order to operate as an actively controlled inertial-based vibration absorber. The pendulum is driven by a brushless motor connected to a programmable digital controller. The floors of the three-story system are instrumented with piezoelectric accelerometers that are connected to the programmable digital controller. Therefore, the torque applied on the pendulum can be actively controlled allowing for the design of a feedback control law based on a real-time estimation of the system state. In order to correctly design the feedback controller and the state estimator, a preliminary mechanical model of the flexible structure is developed employing a lumped parameter approach. After that, a refined mechanical model of the three-story shear building system is derived from input-output experimental data by using a system identification procedure developed in this work. For this purpose, a method for constructing mechanical models from identified state-space representations is used for identifying first-order and second-order dynamical models of the flexible structure. Subsequently, a simple least-square method is employed in order to obtain an improved estimation of the damping model of the flexible structure. The identified mechanical model of the three-story shear building system is effectively used to design a feedback controller and a state estimator by using the Linear Quadratic Gaussian (LQG) control approach. Finally, the numerical procedure developed in the paper is experimentally tested using the three-story shear building model as a demonstrative example in order to verify the effectiveness of the identification and control approach proposed in this investigation.

#### *D. Organization of the Manuscript*

The remaining part of this paper is organized according to the following structure. In Section II, a description of the mechanical system analyzed in this paper is reported. In Section III, a simple lumped parameter model for the three-story shear building system that describes the mechanical vibrations of the flexible structure considered as the case study is developed. In Section IV, the computational steps of the proposed system identification numerical procedure are described. In Section V, the system identification numerical procedure developed in the paper is used to determine a discrete mechanical model of the flexible structure based on input-output experimental measurements. In Section VI, the development and the implementation of the control scheme for reducing the structural vibration of the three-story building system are described. In Section VII, a summary of this investigation and the conclusions drawn in this study are reported.

## II. SYSTEM DESCRIPTION

In this section, a description of the mechanical system analyzed in this investigation is reported. The mechanical system considered as the demonstrative example of the approach developed in the paper is a three-dimensional flexible structure and is shown in figure 1. The flexible structure

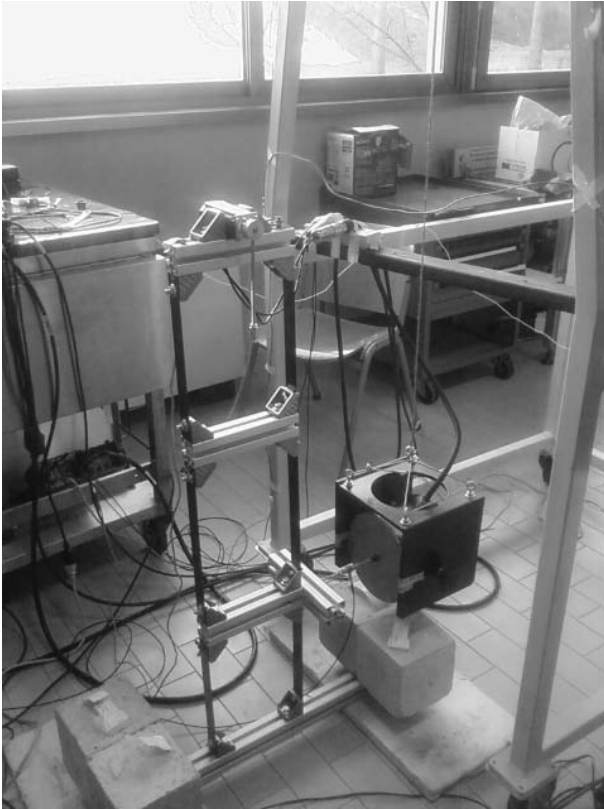


Fig. 1. Experimental test rig.

used as test rig can be modeled as a three-story shear building system. The structural system is composed of six flexible beams and three rigid connecting rods. The flexible beams are made of harmonic steel while the material of the connecting rods is aluminum. The dynamic behavior of the mechanical system considered as a case study is of interest for this investigation and serves as a test rig for studying the mechanical vibrations of real full-scale flexible structures subjected to the earthquake. For this purpose, the frequency range of interest for this study includes all the excitation frequencies between 0 Hz and 15 Hz. In this frequency range, the flexible beams deform as linear elastic continuum bodies and the connecting rods behave essentially as rigid bodies. Observing the geometric configuration of the three-story system, this flexible structure is deployed in a plane. Therefore, the lateral stiffness and the torsional stiffness of the flexible structure are considerably larger than stiffness along the plane. Consequently, this three-dimensional flexible structure can be modeled as a planar three-story shear building system with a very good approximation. The first floor of the flexible structure is excited by a shaker that is connected to the structure by means of a stinger. A load cell is collocated between the first floor and the stinger in order to measure the force transferred to the flexible structure by the shaker. In order to minimize the inertial

influence of the shaker on the flexible structure, the shaker is suspended through a steel cable fixed on an external support isolated from the flexible structure of interest. The shaker is connected to a power amplifier which is controlled by an arbitrary wave function generator. In order to measure the time response of the three-story shear building system, piezoelectric transducers that sense the system accelerations are collocated on each floor of the flexible structure. Furthermore, the flexible structure is actively controlled by using an inertial-based vibration absorber collocated on the third floor. The actively controlled inertial-based vibration absorber is realized by using a physical pendulum having an additional mass concentrated on the pendulum tip as shown in figure 2. The pendulum can oscillate along the

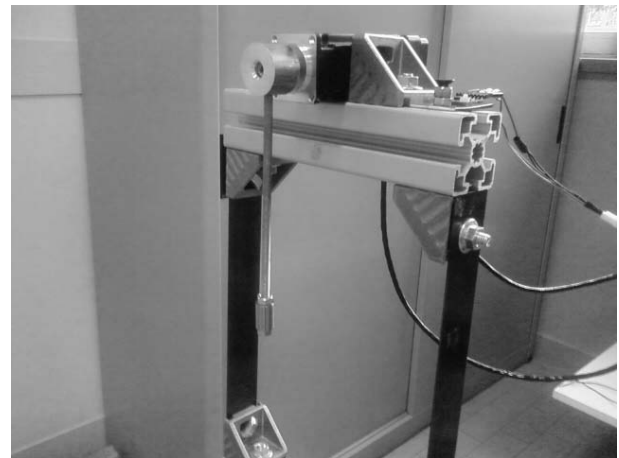


Fig. 2. Actively controlled inertial-based vibration absorber.

same plane in which the flexible structure is deployed in order to contrast the mechanical vibrations of the structural system by means of its inertial effects. The pendulum is actively controlled employing a control actuator driven by a brushless motor. The brushless motor is equipped with an encoder that allows for measuring the pendulum angular displacement. The electromechanical actuator provides a control torque that is computed in real time by using a digital controller that communicates with the brushless motor by means of a drive device. The digital controller reads the acceleration signals coming from the piezoelectric transducers and the force signal measured by the load cell. The digital controller can be programmed and monitored offline in order to calculate a feedback control law for the control torque of the brushless motor based on the force and acceleration measurements. A schematic representation of the identification and control scheme for the test rig is shown in figure 3. A detailed three-dimensional CAD model of the flexible structure together with the actively controlled inertial-based vibration absorber is represented in figure 4. Furthermore, in order to develop an effective control law for the digital controller, an experimental modal analysis of the flexible structure was performed at first. To this end, the three floors of the flexible structure were excited by using an impact hammer instrumented with a load cell connected to a spectrum analyzer. The acceleration signals measured by the piezoelectric transducers in correspondence of the external excitations of the impact hammer were recorded by using the spectrum analyzer in order to obtain the input-

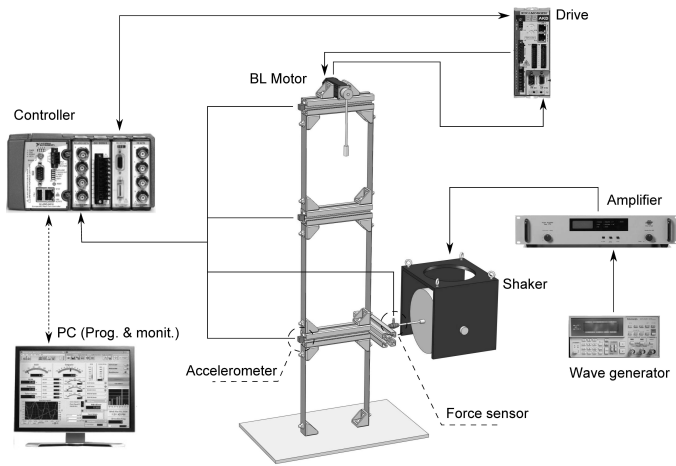


Fig. 3. Identification and control scheme.



Fig. 4. Three-dimensional CAD model of the mechanical system.

output experimental data necessary for the use of system identification numerical procedures [60]–[62].

### III. DYNAMIC MODEL

In this section, a simple lumped parameter model for the three-story shear building system that describes the mechanical vibrations of the flexible structure is developed. The analytical development of this preliminary mechanical model of the flexible structure is necessary in order to guide the subsequent identification process based on experimental measurements. A schematic representation of the lumped parameter model of the flexible structure is shown in figure 5. In the analysis of this preliminary mechanical model, the flexible structure is modeled considering three lumped masses that represent the connecting rods and three spring

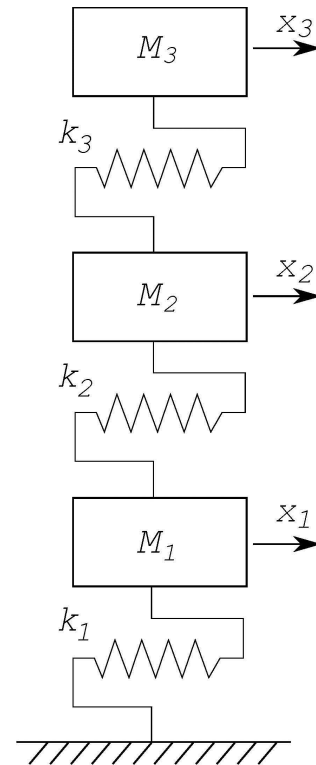


Fig. 5. Lumped parameter model.

elements that represent the flexible beams. On the other hand, the angular displacement of the pendulum is fixed in order to model the behavior of the flexible structure in the case in which the control system is not active. Therefore, the lumped parameter model of the three-story shear building system includes only  $n_2 = 3$  degrees of freedom. Denoting the continuous time with  $t$ , the degrees of freedom of the flexible structure are the horizontal displacements of the system first, second, and third floors respectively indicated as  $x_1(t)$ ,  $x_2(t)$ , and  $x_3(t)$ . Thus, the generalized coordinate vector that identifies the configuration of the three-story shear building model is indicated with  $\mathbf{x}(t)$  and is given by  $\mathbf{x}(t) = [x_1(t) \ x_2(t) \ x_3(t)]^T$ . Since in the frequency range of interest and for the amplitudes of the inputs considered as external excitations the dynamic behavior of the flexible structure is linear, the equations of motion that describe the lumped parameter model of the three-story shear building system can be written in a compact matrix form as  $\mathbf{M}\ddot{\mathbf{x}}(t) + \mathbf{K}\mathbf{x}(t) = \mathbf{0}$ , where  $\ddot{\mathbf{x}}(t)$  is the system generalized acceleration vector,  $\mathbf{x}(t)$  denotes the system generalized coordinate vector,  $\mathbf{M}$  is the system mass matrix, and  $\mathbf{K}$  denotes the system stiffness matrix. In the analytical derivation of the equations of motion of the flexible structure, the effect of the structural damping is neglected. However, a simple but realistic estimation of the viscous damping of the flexible structure will be subsequently obtained in the paper by using the proposed identification procedure. The mass and stiffness matrices of the lumped parameter model for the flexible structure can be readily obtained using the classical methods of analytical dynamics. In particular, the mass matrix is given by  $\mathbf{M} = \text{diag}(m_{1,1}, m_{2,2}, m_{3,3})$ , while

the stiffness matrix is defined as follows:

$$\mathbf{K} = \begin{bmatrix} k_{1,1} & k_{1,2} & 0 \\ k_{1,2} & k_{2,2} & k_{2,3} \\ 0 & k_{2,3} & k_{3,3} \end{bmatrix} \quad (1)$$

It is important to note that the mass matrix  $\mathbf{M}$  and the stiffness matrix  $\mathbf{K}$  of the three-story shear building model are constant, symmetric, and positive-definite matrices. The entries  $m_{i,j}$  and  $k_{i,j}$  for  $i = 1, 2, \dots, n_2$  and  $j = 1, 2, \dots, n_2$  of the system mass and stiffness matrices are given by:

$$\begin{cases} m_{1,1} = m_1 \\ m_{2,2} = m_2 \\ m_{3,3} = m_3 + m_4 \end{cases}, \begin{cases} k_{1,1} = k_1 + k_2, k_{1,2} = -k_2 \\ k_{2,2} = k_2 + k_3, k_{2,3} = -k_3 \\ k_{3,3} = k_3 \end{cases} \quad (2)$$

where  $m_1 = 1.281$  ( $kg$ ),  $m_2 = 0.814$  ( $kg$ ), and  $m_3 = 1.380$  ( $kg$ ) are the masses of the first, second, and third connecting rods, respectively, whereas  $m_4 = 0.083$  ( $kg$ ) is the mass of the pendulum. The stiffness of each flexible beam can be readily computed assuming a set of clamped-clamped boundary conditions and a parallel configuration of the resulting lumped spring elements to yield  $k_1 = 24EJ/L_1^3$ ,  $k_2 = 24EJ/L_2^3$ , and  $k_3 = 24EJ/L_3^3$ , where  $E = 207 \cdot 10^9$  ( $N/m^2$ ) denotes the elastic modulus of the flexible beams,  $J = 2.917 \cdot 10^{-12}$  ( $m^4$ ) represents the second moment of area of the flexible beams, whereas  $L_1 = 23 \cdot 10^{-2}$  ( $m$ ),  $L_2 = 28 \cdot 10^{-2}$  ( $m$ ), and  $L_3 = 23 \cdot 10^{-2}$  ( $m$ ) are the lengths of the first, second, and third flexible beams, respectively. A modal analysis can be readily performed using the lumped parameter model of the three-story building model in order to obtain the system natural frequencies  $f_{n,j}$  and the corresponding modal vectors  $\varphi_j$  associated with the normal mode  $j$  which can be written as  $\varphi_j = e^{i\theta_j} \rho_j$ , where  $e$  is the Napier's constant,  $i = \sqrt{-1}$  is the imaginary unit,  $\rho_j$  denotes the vector of relative amplitudes associated with the mode  $j$ , and  $\theta_j$  represents a diagonal matrix containing the relative phases of the components of the mode  $j$ . Thus, the modal parameters of the flexible structure obtained by using the preliminary three-story shear building lumped parameter model are given by:

$$\begin{cases} f_{n,1} = 1.962 \text{ (Hz)} \\ \rho_1 = [1 \quad 2.509 \quad 3.085]^T \\ \theta_1 = \text{diag}(0, 0, 0) \end{cases} \quad (3)$$

$$\begin{cases} f_{n,2} = 5.780 \text{ (Hz)} \\ \rho_2 = [1 \quad 0.2447 \quad 0.394]^T \\ \theta_2 = \text{diag}(0, 0, -3.141) \end{cases} \quad (4)$$

$$\begin{cases} f_{n,3} = 8.807 \text{ (Hz)} \\ \rho_3 = [1 \quad 3.138 \quad 1.136]^T \\ \theta_3 = \text{diag}(0, -3.141, 0) \end{cases} \quad (5)$$

As expected, the lumped parameter model of the flexible structure leads to a set of three mode shapes where the first normal mode has no nodes, the second normal mode has one node, and the third normal mode has two nodes. The modal parameters obtained by using the simplified mathematical model of the flexible structure will be used to guide and corroborate the numerical results obtained employing the proposed system identification method based on experimental input-output data [63]–[66].

#### IV. SYSTEM IDENTIFICATION METHOD

In this section, the system identification method used in the paper is described. To this end, consider a state-space model of a mechanical system that describes the dynamic behavior of the flexible structure of interest for this investigation. For both linear and nonlinear systems, a state-space model of the dynamic equations of a mechanical system can be obtained by using a continuous-time approach or employing directly a discrete-time representation [67]–[69]. In this investigation, a discrete-time representation is used in order to facilitate the subsequent computer programming of the digital controller. In general, a discrete-time model of a mechanical system is described by a set of dynamic and measurement equations given by:

$$\begin{cases} \mathbf{z}(k+1) = \mathbf{A}\mathbf{z}(k) + \mathbf{B}\mathbf{u}(k) \\ \mathbf{y}(k) = \mathbf{C}\mathbf{z}(k) + \mathbf{D}\mathbf{u}(k) \end{cases} \quad (6)$$

where  $k$  represents the discrete time,  $\mathbf{z}(k)$  is the discrete-time state vector having dimension  $n = 2n_2$ ,  $n_2$  is the number of generalized coordinates of the mechanical system of interest,  $\mathbf{u}(k)$  denotes the discrete-time input vector of dimension  $r$ ,  $\mathbf{y}(k)$  is the discrete-time output vector having dimension  $m$ ,  $\mathbf{A}$  identifies the discrete-time system state matrix of dimension  $n \times n$ ,  $\mathbf{B}$  denotes the discrete-time input influence matrix having dimension  $n \times r$ ,  $\mathbf{C}$  is the output influence matrix of dimension  $m \times n$ , and  $\mathbf{D}$  denotes the direct transmission matrix having dimension  $m \times r$ . These equations respectively represent the time evolution of the system state due to its intrinsic dynamics and to the variation in time of the physical quantities measured by the instrumentation. In order to improve the accuracy of the dynamic analysis, one can introduce a state estimator in the state-space model of the mechanical system described by an observed set of discrete-time dynamic and measurement equations. By doing so, one obtains:

$$\begin{cases} \hat{\mathbf{z}}(k+1) = \bar{\mathbf{A}}\hat{\mathbf{z}}(k) + \bar{\mathbf{B}}\mathbf{v}(k) \\ \hat{\mathbf{y}}(k) = \mathbf{C}\hat{\mathbf{z}}(k) + \mathbf{D}\mathbf{u}(k) \end{cases} \quad (7)$$

where  $\hat{\mathbf{z}}(k)$  is the estimated state vector of dimension  $n$ ,  $\hat{\mathbf{y}}(k)$  represents the estimated measurement vector having dimension  $m$ ,  $\bar{\mathbf{A}}$  denotes the discrete-time observer state matrix of dimension  $n \times n$ ,  $\bar{\mathbf{B}}$  identifies the discrete-time observer state influence matrix having dimension  $n \times (r + m)$ , and  $\mathbf{v}(k)$  is the generalized input vector of dimension  $r + m$ . The matrix and vector quantities  $\bar{\mathbf{A}}$ ,  $\bar{\mathbf{B}}$ , and  $\mathbf{v}(k)$  are respectively defined as follows:

$$\begin{cases} \bar{\mathbf{A}} = \mathbf{A} + \mathbf{G}\mathbf{C} \\ \bar{\mathbf{B}} = [ \mathbf{B} + \mathbf{G}\mathbf{D} \quad -\mathbf{G} ] \\ \mathbf{v}(k) = [ \mathbf{u}^T(k) \quad \mathbf{y}^T(k) ]^T \end{cases} \quad (8)$$

where  $\mathbf{G}$  represents the observer matrix having dimension  $n \times m$ . The observer matrix  $\mathbf{G}$  is aimed at adjusting the eigenvalues of the observer state matrix  $\bar{\mathbf{A}}$  with respect to the eigenvalues of the state matrix  $\mathbf{A}$ . Consequently, the observer state matrix  $\bar{\mathbf{A}}$  can be made asymptotically stable employing an appropriate selection of the observer matrix  $\mathbf{G}$ . Furthermore, for a general linear time-invariant dynamical

system, the input-output relationship of the discrete-time dynamic model represented in the state-space and the recursive sequence of the discrete-time observer state-space model can be respectively written as follows:

$$\begin{cases} \mathbf{y}(k) = \sum_{j=0}^k (\mathbf{Y}_j \mathbf{u}(k-j)) \\ \hat{\mathbf{y}}(k) = \sum_{j=0}^k (\bar{\mathbf{Y}}_j \mathbf{v}(k-j)) \end{cases} \quad (9)$$

where the sequence of matrices  $\mathbf{Y}_k$  is formed by  $m \times r$  rectangular matrices that are known as discrete impulse response functions or system Markov parameters, whereas the sequence of matrices  $\bar{\mathbf{Y}}_k$  is made of  $m \times (r+m)$  rectangular matrices called observer Markov parameters. The sequences of system and observer Markov parameters  $\mathbf{Y}_k$  and  $\bar{\mathbf{Y}}_k$  are respectively defined as follows:

$$\begin{cases} \mathbf{Y}_0 = \mathbf{D} \\ \mathbf{Y}_k = \mathbf{C}\mathbf{A}^{k-1}\mathbf{B} \end{cases}, \quad \begin{cases} \bar{\mathbf{Y}}_0 = \mathbf{D} \\ \bar{\mathbf{Y}}_k = \mathbf{C}\bar{\mathbf{A}}^{k-1}\bar{\mathbf{B}} \end{cases} \quad (10)$$

In order to facilitate the development of an effective numerical procedure for performing in the time domain the system identification of a discrete-time dynamic model represented in the state-space, one can define for a mechanical system the additional sequence of matrices  $\mathbf{Y}_0^0 = \mathbf{D}$  and  $\mathbf{Y}_k^0 = \mathbf{C}\mathbf{A}^{k-1}\mathbf{G}$ , where the matrices  $\mathbf{Y}_k^0$  are  $m \times m$  rectangular matrices that are referred to as observer gain Markov parameters. By using experimental input-output data, the sequence of observer Markov parameters can be obtained using a simple least-square computational approach. This process leads to a sequence of matrices that represent the set of observer Markov parameters identified experimentally. Once that this process has been successfully performed, one can obtain both the set of system Markov parameters and the set of observer gain Markov parameters starting from the identified observer Markov parameters. For this purpose, consider the following input-output representation of a dynamical system described by a discrete-time dynamic model represented in the state-space:

$$\mathbf{y}(k) + \sum_{j=1}^p (\bar{\mathbf{Y}}_j^{(2)} \mathbf{y}(k-j)) = \quad (11)$$

$$\sum_{j=1}^p (\bar{\mathbf{Y}}_j^{(1)} \mathbf{u}(k-j)) + \mathbf{D}\mathbf{u}(k)$$

where  $\bar{\mathbf{Y}}_k^{(1)}$  and  $\bar{\mathbf{Y}}_k^{(2)}$  are rectangular matrices having respectively dimensions  $m \times r$  and  $m \times m$  that are defined as follows:

$$\begin{cases} \bar{\mathbf{Y}}_k^{(1)} = \mathbf{C}(\mathbf{A} + \mathbf{G}\mathbf{C})^{k-1}(\mathbf{B} + \mathbf{G}\mathbf{D}) \\ \bar{\mathbf{Y}}_k^{(2)} = \mathbf{C}(\mathbf{A} + \mathbf{G}\mathbf{C})^{k-1}\mathbf{G} \end{cases} \quad (12)$$

It can easily be proved that the sequence of matrices that represents the observer Markov parameters can be written in a block matrix form as  $\bar{\mathbf{Y}}_k = \begin{bmatrix} \bar{\mathbf{Y}}_k^{(1)} & -\bar{\mathbf{Y}}_k^{(2)} \end{bmatrix}$ . The constant coefficients of the recursive sequence can be numerically calculated using a least-square approach based on input and output experimental data. To this end, a computational

methodology based on the Observer/Kalman Filter Identification Method (OKID) can be readily used. This method allows for computing the sequence of Markov parameters from experimental data employing experimental measurements. Considering a data set having length  $l$ , the recursive relationship can be mathematically expressed in a matrix form as  $\bar{\mathbf{L}}_p = \mathbf{Y}\mathbf{V}_p^+$ , where  $\mathbf{Y}$ ,  $\bar{\mathbf{L}}_p$ , and  $\mathbf{V}_p$  are rectangular matrices respectively of dimensions  $m \times l$ ,  $m \times (r + (r+m)p)$ , and  $(r + (r+m)p) \times l$  that are respectively defined as follows:

$$\begin{cases} \mathbf{Y} = [\mathbf{y}(0) \quad \mathbf{y}(1) \quad \dots \quad \mathbf{y}(l-1)] \\ \bar{\mathbf{L}}_p = [\bar{\mathbf{Y}}_0 \quad \bar{\mathbf{Y}}_1 \quad \dots \quad \bar{\mathbf{Y}}_p] \\ \mathbf{V}_p = \begin{bmatrix} \mathbf{u}(0) & \mathbf{u}(1) & \dots & \mathbf{u}(l-1) \\ \mathbf{0} & \mathbf{v}(0) & \dots & \mathbf{v}(l-2) \\ \vdots & \vdots & \ddots & \vdots \\ \mathbf{0} & \mathbf{0} & \dots & \mathbf{v}(l-p-1) \end{bmatrix} \end{cases} \quad (13)$$

where  $p$  is an integer number that denotes the discrete time at which the estimated output vector  $\hat{\mathbf{y}}(k)$  approaches the actual measured output vector  $\mathbf{y}(k)$ . The sequence of first  $p$  observer Markov parameters  $\bar{\mathbf{Y}}_k$  are included in block matrix  $\bar{\mathbf{L}}_p$ . Therefore, a simple least-square estimation method can be used for obtaining an approximate solution for the observer Markov parameters  $\bar{\mathbf{Y}}_k$  employing experimental input-output measurements as  $\bar{\mathbf{L}}_p = \mathbf{Y}\mathbf{V}_p^+$ , where  $\mathbf{V}_p^+$  represents a rectangular matrix having dimension  $m \times (r + (r+m)p)$  that identifies the Moore-Penrose pseudoinverse matrix corresponding to the matrix  $\mathbf{V}_p$ . By using simple recursive relationships, one can obtain the system Markov parameters and the observer gain Markov parameters using the estimated observer Markov parameters. Subsequently, the combination of the identified system and observer gain Markov parameters, which are denoted respectively as  $\mathbf{Y}_k$  and  $\mathbf{Y}_k^0$ , can be readily used for developing an applied system identification algorithm based on time domain data. For this purpose, a computational procedure based on the Eigensystem Realization Algorithm (ERA) can be employed for deriving a state-space set of characteristic matrices  $\mathbf{A}$ ,  $\mathbf{B}$ ,  $\mathbf{C}$ , and  $\mathbf{D}$ . These matrices characterize the state-space model of a general linear mechanical system obtained using a discrete-time representation based on the system Markov parameters identified from experimental data. To this end, consider the following block matrix that contains the system and observer gain Markov parameters  $\mathbf{P}_k = \begin{bmatrix} \mathbf{Y}_k & \mathbf{Y}_k^0 \end{bmatrix}$ , where  $\mathbf{P}_k$  is a block matrix having dimensions  $m \times (r+m)$ . The identification of the matrix  $\mathbf{P}_k$  is necessary for constructing a generalized block Hankel matrix defined as:

$$\bar{\mathbf{N}}(k-1) = \begin{bmatrix} \mathbf{P}_k & \mathbf{P}_{k+1} & \dots & \mathbf{P}_{k+\delta-1} \\ \mathbf{P}_{k+1} & \mathbf{P}_{k+2} & \dots & \mathbf{P}_{k+\delta} \\ \vdots & \vdots & \ddots & \vdots \\ \mathbf{P}_{k+\gamma-1} & \mathbf{P}_{k+\gamma} & \dots & \mathbf{P}_{k+\gamma+\delta-2} \end{bmatrix} \quad (14)$$

where  $\bar{\mathbf{N}}(k-1)$  denotes a block Hankel matrix having dimensions  $\gamma m \times \delta(r+m)$  in which both the set of system Markov parameters and the set of observer gain Markov parameters  $\mathbf{Y}_k$  and  $\mathbf{Y}_k^0$  are included, while  $\gamma$  and  $\delta$  are two integer parameters that can be assumed as  $\gamma = p$  and  $\delta = l - p$ , where  $l$  is the length of the data set used for the numerical implementation of the system identification

algorithm. Considering the case in which  $k = 0$ , the generalized Hankel matrix  $\bar{\mathbf{N}}(0)$  can be factorized using the Singular Value Decomposition (SVD) and can be written as  $\bar{\mathbf{N}}(0) = \bar{\mathbf{R}}\bar{\mathbf{Q}}\bar{\mathbf{S}}^T$ , where the rectangular matrix  $\bar{\mathbf{Q}}$  contains the singular values of the generalized Hankel matrix  $\bar{\mathbf{N}}(0)$ , while the columns of the matrices  $\bar{\mathbf{R}}$  and  $\bar{\mathbf{S}}$  form orthonormal vectors. In particular, the block matrix  $\bar{\mathbf{Q}}$  can be expressed as  $\bar{\mathbf{Q}} = \text{block} \left[ \begin{array}{c} [\bar{\mathbf{Q}}_{\hat{n}}, \mathbf{O}] \\ [\mathbf{O}, \mathbf{O}] \end{array} \right]$ , where the submatrix  $\bar{\mathbf{Q}}_{\hat{n}}$  is a square diagonal matrix that is given by  $\bar{\mathbf{Q}}_{\hat{n}} = \text{diag}(q_1, q_2, \dots, q_{\hat{n}})$ , where  $q_i, 1 = 1, 2, \dots, \hat{n}$  represent the nonzero singular values associated with the generalized Hankel matrix  $\bar{\mathbf{N}}(0)$ . Indicating respectively with  $\bar{\mathbf{R}}_{\hat{n}}$  and  $\bar{\mathbf{S}}_{\hat{n}}$  the rectangular matrices formed by the first  $\hat{n}$  columns of the rectangular matrices  $\bar{\mathbf{R}}$  and  $\bar{\mathbf{S}}$ , the generalized Hankel matrix  $\bar{\mathbf{N}}(0)$  and its Moore-Penrose pseudoinverse matrix  $\bar{\mathbf{N}}^+(0)$  can be respectively written as  $\bar{\mathbf{N}}(0) = \bar{\mathbf{R}}_{\hat{n}}\bar{\mathbf{Q}}_{\hat{n}}\bar{\mathbf{S}}_{\hat{n}}^T$  and  $\bar{\mathbf{N}}^+(0) = \bar{\mathbf{S}}_{\hat{n}}\bar{\mathbf{Q}}_{\hat{n}}^{-1}\bar{\mathbf{R}}_{\hat{n}}^T$ . The analysis of the spectrum of the singular values  $q_i, 1 = 1, 2, \dots, \hat{n}$  of the generalized Hankel matrix  $\bar{\mathbf{N}}(0)$  allows for determining the order  $\hat{n}$  of the identified dynamical model of the mechanical system under consideration based on the sequences of input-output data. By doing so, an identified discrete-time dynamic model represented in the state-space associated with the mechanical system under consideration is given by the discrete-time state-space matrices  $\hat{\mathbf{A}}, \hat{\mathbf{B}}, \hat{\mathbf{C}},$  and  $\hat{\mathbf{D}}$  as well as by the observer matrix  $\hat{\mathbf{G}}$  resulting from the system identification algorithm. Thus, one can obtain the identified discrete-time dynamic model in the state-space of the dynamical system under consideration employing the following equations:

$$\left\{ \begin{array}{l} \hat{\mathbf{A}} = \bar{\mathbf{Q}}_{\hat{n}}^{-1/2} \bar{\mathbf{R}}_{\hat{n}}^T \bar{\mathbf{N}}(1) \bar{\mathbf{S}}_{\hat{n}} \bar{\mathbf{Q}}_{\hat{n}}^{-1/2} \\ [\hat{\mathbf{B}} \quad \hat{\mathbf{G}}] = \bar{\mathbf{Q}}_{\hat{n}}^{-1/2} \bar{\mathbf{S}}_{\hat{n}}^T \mathbf{E}_{r+m} \\ \hat{\mathbf{C}} = \mathbf{E}_m^T \bar{\mathbf{R}}_{\hat{n}} \bar{\mathbf{Q}}_{\hat{n}}^{-1/2} \\ \hat{\mathbf{D}} = \mathbf{Y}_0 = \bar{\mathbf{Y}}_0 \end{array} \right. \quad (15)$$

where  $\mathbf{E}_m$  and  $\mathbf{E}_{r+m}$  are Boolean matrices with appropriate dimensions. The set of identified matrices  $\hat{\mathbf{A}}, \hat{\mathbf{B}}, \hat{\mathbf{C}}, \hat{\mathbf{D}},$  and  $\hat{\mathbf{G}}$  represents a minimum order, controllable, and observable state-space realization of a general mechanical system having a linear mathematical structure. In particular, although the numerical values of the entries of the identified characteristic matrices  $\hat{\mathbf{A}}, \hat{\mathbf{B}}, \hat{\mathbf{C}},$  and  $\hat{\mathbf{D}}$  are not equal to those of the actual discrete-time dynamic model represented in the state-space of the mechanical system given by  $\mathbf{A}, \mathbf{B}, \mathbf{C},$  and  $\mathbf{D}$ , the modal parameters of the identified mechanical model coincide with the actual modal parameters of the dynamical system [70], [71]. Moreover, the discrete-time dynamic model represented in the state-space of the mechanical system can be readily transformed in its continuous-time counterpart. Denoting with  $\hat{\mathbf{L}}_c$  the diagonal matrix containing the eigenvalues of the continuous-time state-space model and indicating with  $\hat{\mathbf{W}}$  the matrix of eigenvectors associated with the system generalized coordinates, a second-order mechanical model of the dynamical system can be derived by using the identified modal parameters of the state-

space model as follows:

$$\left\{ \begin{array}{l} \hat{\mathbf{M}} = \left( \hat{\mathbf{W}} \hat{\mathbf{L}}_c \hat{\mathbf{W}}^T \right)^{-1} \\ \hat{\mathbf{K}} = - \left( \hat{\mathbf{W}} \hat{\mathbf{L}}_c^{-1} \hat{\mathbf{W}}^T \right)^{-1} \\ \hat{\mathbf{R}} = - \left( \hat{\mathbf{M}} \hat{\mathbf{W}} \hat{\mathbf{L}}_c^2 \hat{\mathbf{W}}^T \hat{\mathbf{M}} \right) \end{array} \right. \quad (16)$$

where  $\hat{\mathbf{M}}$  is the identified mass matrix,  $\hat{\mathbf{K}}$  represents the identified stiffness matrix, and  $\hat{\mathbf{R}}$  denotes the identified damping matrix of the mechanical system under study. However, the estimate values of the entries of the system damping matrix  $\hat{\mathbf{R}}$  are considerably influenced by the noise that affects the input-output data set. For lightly damped mechanical systems, an improved estimation of the identified damping matrix of the mechanical system can be obtained by using the proportional damping assumption given by  $\mathbf{R} = \alpha \mathbf{M} + \beta \mathbf{K}$ . By doing so, one can employ a least-square approach for the estimation of the proportional damping coefficients  $\hat{\alpha}$  and  $\hat{\beta}$  which characterize the the proportional damping hypothesis. To this end, the improved estimation of the system damping matrix  $\hat{\mathbf{R}}$  can be written as  $\hat{\mathbf{R}} = \hat{\alpha} \hat{\mathbf{M}} + \hat{\beta} \hat{\mathbf{K}}$ , where the estimated proportional damping coefficients  $\hat{\alpha}$  and  $\hat{\beta}$  can be obtained using the a least-square approach given by  $\bar{\mathbf{x}} = \bar{\mathbf{A}}_f^+ \bar{\mathbf{b}}_\xi$ , where  $\bar{\mathbf{x}} = [\hat{\alpha} \quad \hat{\beta}]^T$ ,  $\bar{\mathbf{b}}_\xi = [\hat{\xi}_1 \quad \hat{\xi}_2 \quad \dots \quad \hat{\xi}_{\hat{n}_2}]^T$ , and:

$$\bar{\mathbf{A}}_f = \frac{1}{2} \begin{bmatrix} \frac{1}{2\pi \hat{f}_{n,1}} & 2\pi \hat{f}_{n,1} \\ \frac{1}{2\pi \hat{f}_{n,2}} & 2\pi \hat{f}_{n,2} \\ \vdots & \vdots \\ \frac{1}{2\pi \hat{f}_{n,\hat{n}_2}} & 2\pi \hat{f}_{n,\hat{n}_2} \end{bmatrix} \quad (17)$$

where  $\bar{\mathbf{A}}_f^+$  denotes the Moore-Penrose pseudoinverse matrix of the coefficient matrix  $\bar{\mathbf{A}}_f$ ,  $\hat{f}_{n,j}$  represents the identified natural frequency associated with the mode  $j$  of the mechanical system, and  $\hat{\xi}_j$  is the identified damping ratio relative to the mode  $j$  of the linear dynamical system [72]–[76].

## V. EXPERIMENTAL INVESTIGATION

In this section, the system identification numerical procedure developed in the paper is used to determine a discrete mechanical model of the flexible structure based on input-output experimental measurements. The numerical results proposed in this section are obtained using a simple computer program coded in MATLAB, while the experimental results reported in this section are obtained by means of the experimental apparatus described previously in the paper. For this purpose, an impact hammer instrumented with a load cell was used to excite impulsively the first floor of the three-story shear building system and the corresponding accelerations of the three floors of the flexible structure were recorded using piezoelectric transducers. The force signal recorded by the load cell of the impact hammer is shown in figure 6. The acceleration signals of the floors of the flexible structure are recorded by the piezoelectric transducers placed on each floor and are respectively shown in figures 7, 8, and 9. The time span considered is  $T_s = 64$  (s) while the sampling frequency used for acquiring the experimental data is  $f_s = 32$  (Hz). Thus, the sampling time step is  $\Delta t = 3.125 \cdot 10^{-2}$  (s) and

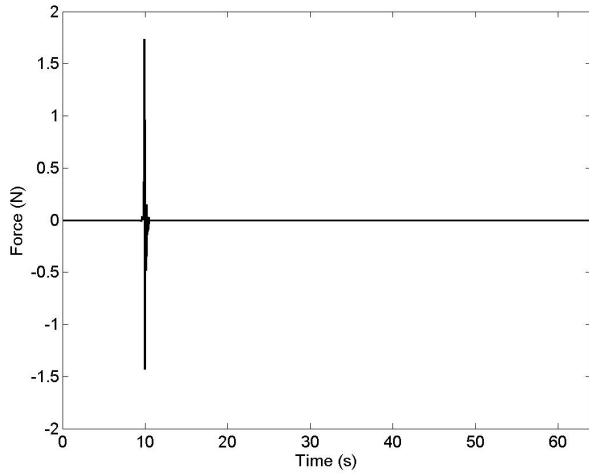


Fig. 6. Force input measurement.

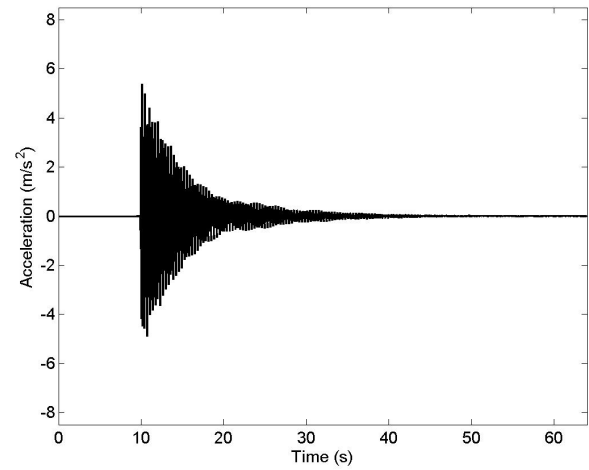


Fig. 8. Acceleration output measurement of the second floor.

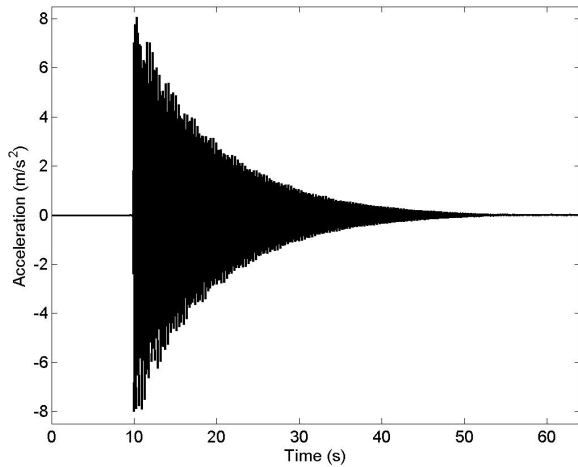


Fig. 7. Acceleration output measurement of the first floor.

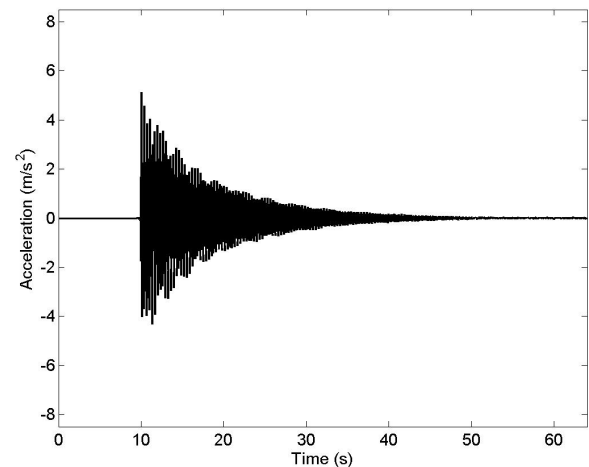


Fig. 9. Acceleration output measurement of the third floor.

the corresponding Nyquist frequency is  $f_N = 16$  (Hz). By using this set of parameters for acquiring the experimental measurements, the frequency range of interest from 0 Hz to 15 Hz is correctly captured by the experimental data. Furthermore, the set of input and output data was first filtered in the time domain and subsequently in the frequency domain. In the time domain, since the action of the impact hammer took place around  $t = 10$  (s), the sections of the input and out signals before  $t = 10$  (s) were set equal to zero because the information contained in this interval of the measured data had no physical meaning. In the frequency domain, a low-pass Butterworth filter having a cut-off frequency of  $f_c = 16$  (Hz) was used in order to eliminate the effect of high-frequency noise. The proposed identification procedure was applied to the set of input-output data obtained by means of experimental measurements. By doing so, the system Markov parameters  $\mathbf{Y}_k$  and the observer gain Markov parameters  $\mathbf{Y}_k^0$  were recovered from the identified sequence of the observer Markov parameters  $\hat{\mathbf{Y}}_k$ . The identified Markov parameters  $\hat{\mathbf{Y}}_k$  and the identified observer gain Markov parameters  $\hat{\mathbf{Y}}_k^0$  were used to construct the matrix sequence of the combined Markov parameters  $\mathbf{P}_k$ . The combined Markov parameters

$\mathbf{P}_k$  were used to assemble the sequence of Hankel matrices  $\bar{\mathbf{N}}(k-1)$  based on experimental data. In particular, a SVD of the Hankel matrix  $\bar{\mathbf{N}}(0)$  was computed and figure 10 shows the magnitude of the identified singular values. As expected, figure 10 shows that only 6 singular values have a relatively large magnitude and, consequently, the order of the identified state-space model that mathematically represent the three-story shear building system is  $\hat{n} = 6$ . Subsequently, the identified discrete-time state-space matrices  $\hat{\mathbf{A}}$ ,  $\hat{\mathbf{B}}$ ,  $\hat{\mathbf{C}}$ ,  $\hat{\mathbf{D}}$ , and  $\hat{\mathbf{G}}$  representing the identified linear dynamical model of the flexible structure and the identified observer matrix were computed yielding to the following set of identified modal parameters:

$$\begin{cases} \hat{f}_{n,1} = 1.934 \text{ (Hz)}, & \hat{\xi}_1 = 0.0395 \\ \hat{\rho}_1 = [1 \quad 2.503 \quad 2.851]^T \\ \hat{\theta}_1 = \text{diag}(0, -0.0186, -0.1053) \end{cases} \quad (18)$$

$$\begin{cases} \hat{f}_{n,2} = 5.690 \text{ (Hz)}, & \hat{\xi}_2 = 0.0030 \\ \hat{\rho}_2 = [1 \quad 0.1492 \quad 0.4221]^T \\ \hat{\theta}_2 = \text{diag}(0, -0.0365, -3.170) \end{cases} \quad (19)$$

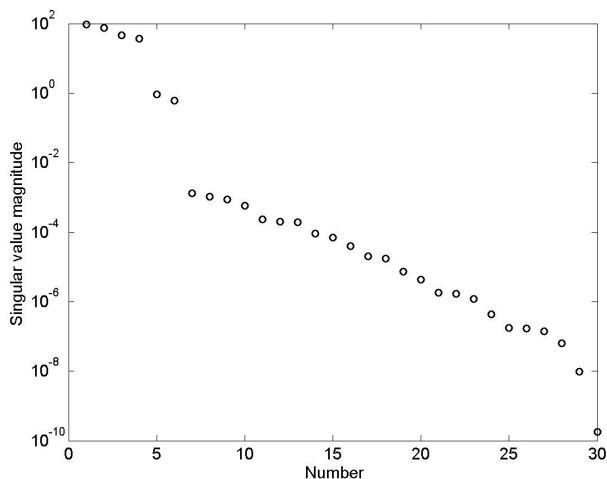


Fig. 10. Magnitude of the singular values of the identified Hankel matrix.

$$\begin{cases} \hat{f}_{n,3} = 8.793 \text{ (Hz)}, & \hat{\xi}_3 = 0.0042 \\ \hat{\rho}_3 = [1 \quad 3.443 \quad 1.476]^T \\ \hat{\theta}_3 = \text{diag}(0, -3.144, -0.0296) \end{cases} \quad (20)$$

where  $\hat{f}_{n,j}$  is the identified natural frequency of the mode  $j$ ,  $\hat{\xi}_j$  denotes the identified damping ratio corresponding to the mode  $j$ ,  $\hat{\varphi}_j = e^{i\hat{\theta}_j} \hat{\rho}_j$  represents the identified modal vector of the normal mode  $j$ ,  $\hat{\rho}_j$  is the identified vector of relative modal amplitudes of the mode  $j$ , and  $\hat{\theta}_j$  represents the relative phase matrix of the mode  $j$ . Figures 11, 12, and 13 respectively show the first, second, and third mode shapes identified by using the computational procedure developed in the paper. It is important to note that the

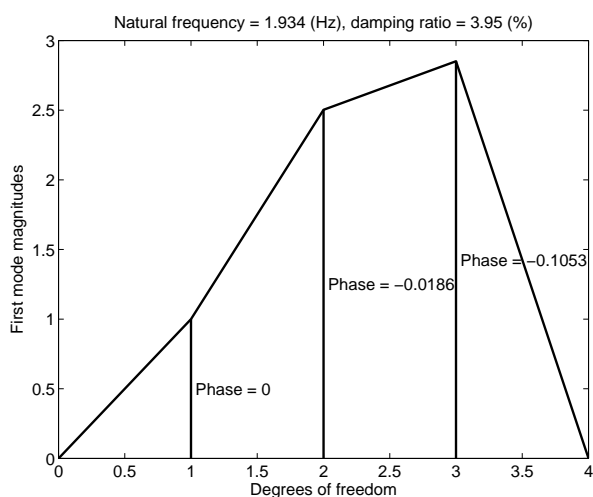


Fig. 11. Identified first mode shape.

modal parameters of the identified continuous-time state-space model are consistent with those obtained by using the preliminary lumped parameter model. Since the identified modal damping is small, the identified mode shapes are approximately in phase or out of phase. Therefore, the hypothesis of proportional damping can be assumed and the proposed method for identifying the proportional damping

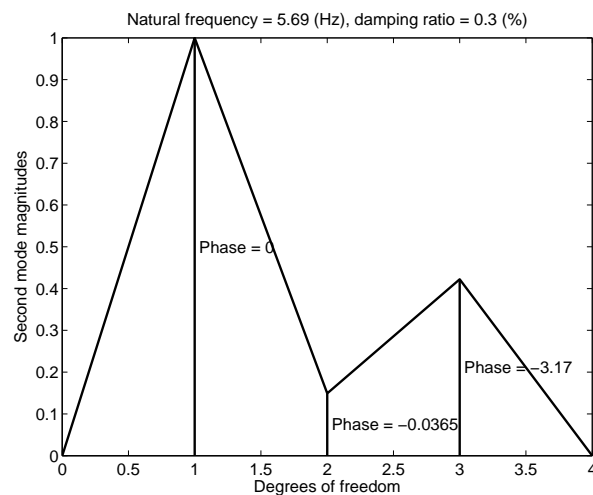


Fig. 12. Identified second mode shape.

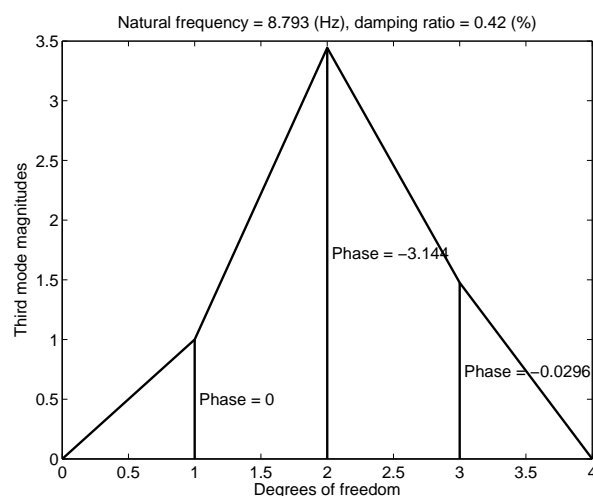


Fig. 13. Identified third mode shape.

coefficients can be applied to yield:

$$\hat{\alpha} = 0.9751, \quad \hat{\beta} = -2.8815 \cdot 10^{-4} \quad (21)$$

where  $\hat{\alpha}$  and  $\hat{\beta}$  denote the identified proportional damping coefficients. Furthermore, a second-order physical model can be constructed from the identified mathematical state-space representation by using the algorithm discussed in the paper to yield:

$$\hat{\mathbf{M}} = \begin{bmatrix} 0.3871 & -0.0156 & 0.0011 \\ -0.0156 & 0.2621 & -0.0323 \\ 0.0011 & -0.0323 & 0.3790 \end{bmatrix} \quad (22)$$

$$\hat{\mathbf{K}} = \begin{bmatrix} 534.061 & -221.931 & 25.696 \\ -221.931 & 614.564 & -432.792 \\ 25.696 & -432.792 & 422.005 \end{bmatrix} \quad (23)$$

$$\hat{\mathbf{R}} = \begin{bmatrix} 9.960 & -4.823 & 1.018 \\ -4.823 & 12.480 & -8.366 \\ 1.018 & -8.366 & 7.017 \end{bmatrix} \quad (24)$$

where  $\hat{\mathbf{M}}$  is the identified mass matrix,  $\hat{\mathbf{K}}$  denotes the identified stiffness matrix, and  $\hat{\mathbf{R}}$  represents the identified damping matrix. An improved estimation of the identified damping matrix  $\hat{\mathbf{R}}$  can be obtained by using the proportional

damping assumption and employing the identified proportional damping coefficients  $\hat{\alpha}$  and  $\hat{\beta}$  as well as the identified mass and stiffness matrices  $\hat{\mathbf{M}}$  and  $\hat{\mathbf{K}}$  as follows:

$$\hat{\mathbf{R}} = \hat{\alpha}\hat{\mathbf{M}} + \hat{\beta}\hat{\mathbf{K}} = \begin{bmatrix} 0.22356 & 0.0487 & -0.0063 \\ 0.0487 & 0.0785 & 0.0932 \\ -0.0063 & 0.0932 & 0.2480 \end{bmatrix} \quad (25)$$

The identified second-order mechanical model of the flexible structure will be used in the paper for designing an effective control strategy for reducing the system vibrations induced by external excitations [77]–[80].

## VI. CONTROL DEVELOPMENT

In this section, the development and the implementation of the control scheme for reducing the structural vibration of the three-story building system are described. For this purpose, the Linear Quadratic Gaussian (LQG) control approach is employed by using the identified second-order mechanical model of the flexible structure. Thus, the design of the control system based on the Linear Quadratic Gaussian (LQG) regulation methodology is performed by combining the identified second-order model of the vibrating structure with a linear lumped parameter model of the actuated pendulum that works as an actively controlled inertial-based vibration absorber. Therefore, the resulting mechanical model used to design the control system includes  $n_2 = 4$  degrees of freedom contained in a new generalized coordinate vector  $\mathbf{x}(t)$  given by  $\mathbf{x}(t) = [x_1(t) \ x_2(t) \ x_3(t) \ \varphi(t)]^T$ , where  $x_1(t)$ ,  $x_2(t)$ , and  $x_3(t)$  represent the linear displacements of the system first, second, and third floors, respectively, while  $\varphi(t)$  identifies the angular displacement of the actively controlled pendulum that serves as an inertial-based vibration absorber. By using the analytical methods of classical mechanics, the mechanical model of the three-story shear building system with the pendulum hinged on the third floor can be mathematically expressed as  $\mathbf{M}\ddot{\mathbf{x}}(t) + \mathbf{R}\dot{\mathbf{x}}(t) + \mathbf{K}\mathbf{x}(t) = \mathbf{B}_{2,e}\mathbf{u}_e(t) + \mathbf{B}_{2,c}\mathbf{u}_c(t)$ , where  $\ddot{\mathbf{x}}(t)$  is the system generalized acceleration vector,  $\dot{\mathbf{x}}(t)$  represents the system generalized velocity vector,  $\mathbf{x}(t)$  denotes the system generalized coordinate vector,  $\mathbf{M}$  is the system mass matrix,  $\mathbf{R}$  represents the system damping matrix,  $\mathbf{K}$  denotes the system stiffness matrix,  $\mathbf{u}_e(t)$  is the vector of uncontrollable inputs,  $\mathbf{u}_c(t)$  is the vector of controllable inputs,  $\mathbf{B}_{2,e}$  is a Boolean matrix that identifies the locations of the uncontrollable inputs, and  $\mathbf{B}_{2,c}$  is a Boolean matrix that identifies the locations of the controllable inputs. The system mass, damping, and stiffness matrices of the flexible structure combined with the actively controlled inertial-based vibration absorber are respectively defined as follows:

$$\begin{cases} \mathbf{M} = \mathbf{B}_x^T \hat{\mathbf{M}} \mathbf{B}_x + \mathbf{B}_4^T \mathbf{M}_4 \mathbf{B}_4 \\ \mathbf{K} = \mathbf{B}_x^T \hat{\mathbf{K}} \mathbf{B}_x + \mathbf{B}_4^T \mathbf{K}_4 \mathbf{B}_4 \\ \mathbf{R} = \mathbf{B}_x^T \hat{\mathbf{R}} \mathbf{B}_x + \mathbf{B}_4^T \mathbf{R}_4 \mathbf{B}_4 \end{cases} \quad (26)$$

where  $\hat{\mathbf{M}}$ ,  $\hat{\mathbf{R}}$ , and  $\hat{\mathbf{K}}$  denote respectively the identified mass, damping, and stiffness matrices, while  $\mathbf{M}_4$ ,  $\mathbf{R}_4$ , and  $\mathbf{K}_4$  represent respectively the mass, damping, and stiffness matrices associated with the actively controlled pendulum

given by:

$$\mathbf{M}_4 = \begin{bmatrix} m_4 & m_4 L_4 \\ m_4 L_4 & m_4 L_4^2 + I_{zz,4} \end{bmatrix} \quad (27)$$

$$\mathbf{K}_4 = m_4 g L_4, \quad \mathbf{R}_4 = 0 \quad (28)$$

where  $g = 9.81 \text{ (m/s}^2\text{)}$  represents the gravity acceleration,  $L_4 = 8.25 \cdot 10^{-2} \text{ (m)}$  is half the length of the pendulum,  $m_4 = 0.083 \text{ (kg)}$  denotes the pendulum mass, and  $I_{zz,4} = 8.32 \cdot 10^{-4} \text{ (kg} \cdot \text{m}^2\text{)}$  identifies the mass moment of inertia of the pendulum referred to its center of mass. The matrices  $\mathbf{B}_x$  and  $\mathbf{B}_4$ , on the other hand, are appropriate Boolean matrices that serve for assembling the mechanical model of the flexible structure with the actively controlled pendulum. For the three-story shear building system, the vector of uncontrollable inputs  $\mathbf{u}_e(t)$  contains an external excitation force applied on the first floor of the three-story shear building system, whereas the vector of controllable inputs  $\mathbf{u}_c(t)$  includes a control torque applied on the pendulum that works as a vibration absorber. The Boolean matrices  $\mathbf{B}_{2,e}$  and  $\mathbf{B}_{2,c}$  respectively identify the locations of the input actions  $\mathbf{u}_e(t)$  and  $\mathbf{u}_c(t)$ . In the experimental testing, the uncontrollable input vector  $\mathbf{u}_e(t)$  is equal to an external force  $F_e(t)$  defined by the superposition of three harmonic components having considerable amplitudes and characterized by a set of excitation frequencies close to the first three natural frequencies of the flexible structure. Furthermore, a noise excitation source is considered in order to simulate the earthquake in the worst case scenario in which external excitation frequencies are close to the system natural frequencies. Therefore, the external force  $F_e(t)$  considered as an uncontrollable input is defined as  $F_e(t) = F_{0,1} \sin(2\pi f_1 t) + F_{0,2} \sin(2\pi f_2 t) + F_{0,3} \sin(2\pi f_3 t)$ , where  $F_{0,1} = 0.1 \text{ (N)}$ ,  $F_{0,2} = 0.1 \text{ (N)}$ , and  $F_{0,3} = 0.1 \text{ (N)}$  are the amplitudes of the first, second, and third harmonic forces, respectively, while  $f_1 = 1.9 \text{ (Hz)}$ ,  $f_2 = 5.7 \text{ (Hz)}$ , and  $f_3 = 8.8 \text{ (Hz)}$  represent the frequencies of the first, second, and third harmonic forces, respectively. The external excitation force can be measured using a load cell collocated between the shaker and the stinger connected with the first floor of the flexible structure. On the other hand, the measurable output variables of the three-story shear building system are the accelerations of the three floors and the angular displacement of the actively controlled pendulum. These output variables are included in a output vector  $\mathbf{y}(t)$  given by  $\mathbf{y}(t) = [\ddot{x}_1(t) \ \ddot{x}_2(t) \ \ddot{x}_3(t) \ \varphi(t)]^T$ . Consequently, the set of measurement equations can be readily written as  $\mathbf{y}(t) = \mathbf{C}_d \mathbf{x}(t) + \mathbf{C}_v \dot{\mathbf{x}}(t) + \mathbf{C}_a \ddot{\mathbf{x}}(t)$ , where  $\mathbf{C}_d$  is the generalized displacement influence matrix on the measured output,  $\mathbf{C}_v$  is the generalized velocity influence matrix on the measured output, and  $\mathbf{C}_a$  is the generalized acceleration influence matrix on the measured output. Considering a time span equal to  $T_s = 64 \text{ (s)}$  and a time step equal to  $\Delta t = 3.125 \cdot 10^{-2} \text{ (s)}$ , an optimal state estimator and an optimal controller can be obtained by using the LQG approach leading to the following set of discrete-time state-space equations:

$$\begin{cases} \hat{\mathbf{z}}(k+1) = \mathbf{A}\hat{\mathbf{z}}(k) + \mathbf{B}_e \mathbf{u}_e(k) + \mathbf{B}_c \mathbf{F}_\infty \hat{\mathbf{z}}(k) \\ \quad \quad \quad + \mathbf{K}_\infty (\mathbf{y}(k) - \hat{\mathbf{y}}(k)) \\ \hat{\mathbf{y}}(k) = \mathbf{C}\hat{\mathbf{z}}(k) + \mathbf{D}_e \mathbf{u}_e(k) + \mathbf{D}_c \mathbf{F}_\infty \hat{\mathbf{z}}(k) \end{cases} \quad (29)$$

where  $\hat{z}(k)$  is the estimated discrete-time state vector and  $\hat{y}(k)$  denotes the estimated discrete-time measurement vector. The discrete-time dynamic model represented in the state-space given by the set of matrices  $\mathbf{A}$ ,  $\mathbf{B}_e$ ,  $\mathbf{B}_c$ ,  $\mathbf{C}$ ,  $\mathbf{D}_e$ , and  $\mathbf{D}_c$  can be easily derived from the mechanical model of the flexible structure combined with the actively controlled inertial-based vibration absorber. Moreover, the matrices  $\mathbf{K}_\infty$  and  $\mathbf{F}_\infty$  represent respectively a discrete-time infinite-horizon Kalman filter gain and a discrete-time infinite-horizon optimal feedback gain which can be readily computed by using the LQG method. In order to analyze the dynamic behavior of the three-story shear building system with and without the action of the control system, the control actuator is deactivated in the time range between  $t = 0$  (s) and  $t = 32$  (s), while the control actuator is activated in the time range between  $t = 32$  (s) and  $t = 64$  (s). Figures 14, 15, and 16 show, respectively, the estimated displacements of the first, second, and third floors of the flexible structure resulting from the implementation of the control system. Figure 17 shows the control torque used

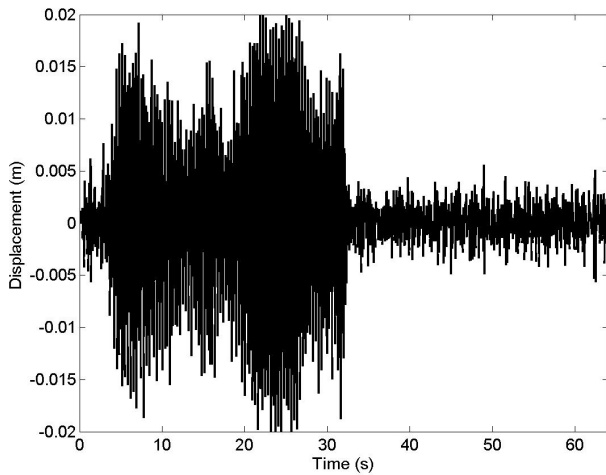


Fig. 14. Estimated displacement of the first floor.

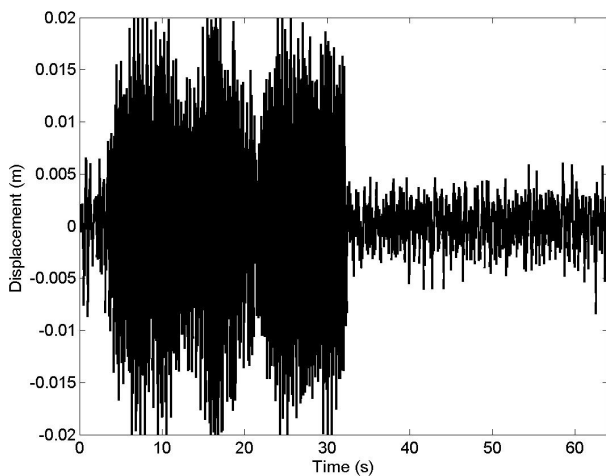


Fig. 15. Estimated displacement of the second floor.

as a controllable input signal for the mechanical system

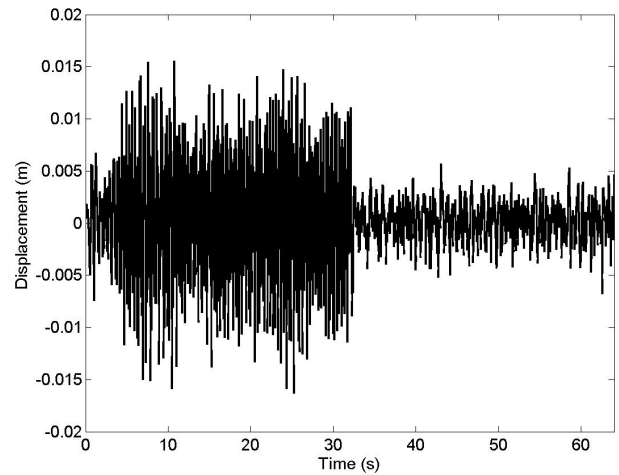


Fig. 16. Estimated displacement of the third floor.

that forms the actively controlled inertial-based vibration absorber. It is apparent from the estimated displacements

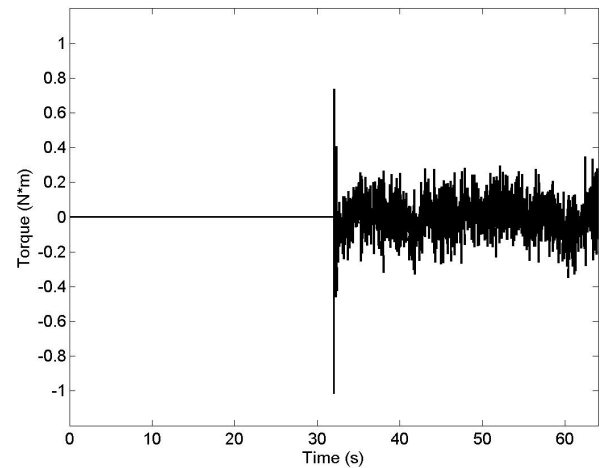


Fig. 17. Control torque

shown in figures 14, 15, and 16 that the action of the control system allows for obtaining a large amplitude reduction of the system mechanical vibrations. In fact, the reduction of the system vibrations can be estimated quantitatively by comparing the maximum amplitude values of the system displacements with and without the action of the vibration absorber as follows:

$$\begin{cases} (x_{1,\max}^u - x_{1,\max}^c)/x_{1,\max}^u = 74.82\ (\%) \\ (x_{2,\max}^u - x_{2,\max}^c)/x_{2,\max}^u = 63.91\ (\%) \\ (x_{3,\max}^u - x_{3,\max}^c)/x_{3,\max}^u = 58.40\ (\%) \end{cases} \quad (30)$$

where  $x_{1,\max}^u$ ,  $x_{2,\max}^u$ , and  $x_{3,\max}^u$  denote the maximum absolute values of the estimated displacements when there is no control action, whereas  $x_{1,\max}^c$ ,  $x_{2,\max}^c$ , and  $x_{3,\max}^c$  represent the maximum absolute values of the estimated displacements when the actively controlled inertial-based vibration absorber acts on the three-story shear building. It can be noticed

that the numerical results found by using the state estimator and employed for assessing the amplitude reductions of the mechanical vibrations of the flexible structure are consistent with the system actual dynamic behavior observed in the experimental testing [81], [82].

## VII. SUMMARY AND CONCLUSIONS

The principal topics of interest for the research of the authors are nonlinear control, multibody dynamics, and system identification [83]–[86]. Thus, the research efforts of the authors are devoted to the development of new optimal control actions for dynamical systems, new methods for obtaining accurate analytical modelling of rigid-flexible multibody mechanical systems, and new numerical parameter identification approaches based on experimental data [87]–[90]. This investigation deals with the development of a new actively controlled inertial-based vibration absorber suitable for controlling the mechanical vibrations of flexible structures. To this end, a system identification method based on the time domain is developed in the paper. For this purpose, the set of the system Markov parameters is used in the paper for obtaining from experimental data the modal parameters of structural systems and, at the same time, in order to derive reliable first-order state-space and second-order mechanical models driven from input-output measurements. Furthermore, a least square estimation method for improving the estimation of the system structural damping is also proposed in this work. Subsequently, a methodology for reducing the system mechanical vibrations induced by external excitation sources by using an actively controlled inertial-based vibration absorber is developed in the paper. The proposed inertial-based vibration absorber is realized by using an actively controlled pendulum system mounted on the third floor of the flexible structure. This device is programmed with both an optimal feedback controller and an optimal state observer. The optimal closed-loop controller and the optimal state estimator were designed by using the Linear Quadratic Gaussian (LQG) algorithm. In order to achieve this goal, the dynamic parameters obtained from the application of the system identification numerical procedure developed in this work were used. Moreover, the proposed approach is corroborated by means of dynamic simulations carried out by using a computer code developed in MATLAB and is experimentally verified employing a simple test rig. In particular, the analytical derivation and the experimental testing of the active control strategy developed in this work for reducing the vibrations of flexible structures are carried out in two steps. In the first step of the analysis, the flexible structure is modeled as a three-story shear building system mathematically represented by using a three-degree-of-freedom lumped parameter model obtained by means of the analytical methods of classical mechanics. Once that an accurate mechanical model was obtained in the first step of the present analysis, an optimal feedback controller and an optimal state estimator were designed in the second part of this work considering the identified state-space and configuration-space dynamic models obtained by using the system identification approach elaborated in the paper. Numerical results and experimental measurements showed that the action of the actively controlled inertial-based vibration absorber leads to a considerable reduction of the vibrations

of the flexible structure considered as the case study. The numerical and experimental results obtained in this paper also demonstrated that the use of applied system identification numerical techniques can considerably facilitate the development of effective control systems for reducing the externally induced vibrations of machines, mechanisms, and structures. Future research will be devoted to the experimental testing of the proposed methodology in the case of the active vibration control problem of complex three-dimensional mechanical systems.

## REFERENCES

- [1] L. Ljung, "Perspectives on System Identification," *Annual Reviews in Control*, vol. 34, no. 1, pp. 1-12, 2010.
- [2] O. Nelles, *Nonlinear System Identification: From Classical Approaches to Neural Networks and Fuzzy Models*, Springer Science and Business Media, 2013.
- [3] T. Sands, "Nonlinear-Adaptive Mathematical System Identification," *Computation*, vol. 5, no. 4, 47, 2017.
- [4] B. Peeters and G. De Roeck, "Stochastic System Identification for Operational Modal Analysis: a Review," *Journal of Dynamic Systems, Measurement, and Control*, vol. 123, no. 4, pp. 1-9, 2001.
- [5] E. Reynders, "System Identification Methods for (Operational) Modal Analysis: Review and Comparison," *Archives of Computational Methods in Engineering*, vol. 19, no. 1, pp. 51-124, 2012.
- [6] Y. Gao, F. Vilecco, M. Li, and W. Song, "Multi-Scale Permutation Entropy based on Improved LMD and HMM for Rolling Bearing Diagnosis," *Entropy*, vol. 19, no. 4, 176, 2017.
- [7] F. Vilecco and A. Pellegrino, "Evaluation of Uncertainties in the Design Process of Complex Mechanical Systems," *Entropy*, vol. 19, no. 9, 475, 2017.
- [8] F. Vilecco and A. Pellegrino, "Entropic Measure of Epistemic Uncertainties in Multibody System Models by Axiomatic Design," *Entropy*, vol. 19, no. 7, 291, 2017.
- [9] R. Castro-Garcia, K. Tiels, O. M. Agudelo, and J. A. Suykens, "Hammerstein System Identification through Best Linear Approximation Inversion and Regularisation," *International Journal of Control*, pp. 1-17, 2017.
- [10] F. P. Carli, T. Chen, and L. Ljung, "Maximum Entropy Kernels for System Identification," *IEEE Transactions on Automatic Control*, vol. 62, no. 3, pp. 1471-1477, 2017.
- [11] T. A. Catanach and J. L. Beck, "Bayesian System Identification using Auxiliary Stochastic Dynamical Systems," *International Journal of Non-Linear Mechanics*, vol. 94, pp. 72-83, 2017.
- [12] D. Belmonte, M. D. L. Dalla Vedova, and P. Maggiore, "Aircraft Flap Control System: Proposal of a Simulink Test Bench for Evaluating Innovative Asymmetry Monitoring and Control Techniques," *International Journal of Mathematical Models and Methods in Applied Sciences*, vol. 10, pp. 51-61, 2016.
- [13] X. Hong, R. J. Mitchell, S. Chen, C. J. Harris, K. Li, and G. W. Irwin, "Model Selection Approaches for Non-linear System Identification: a Review," *International Journal of Systems Science*, vol. 39, no. 10, pp. 925-946, 2008.
- [14] H. Unbehauen and G. P. Rao, "A Review of Identification in Continuous-time Systems," *Annual Reviews in Control*, vol. 22, pp. 145-171, 1998.
- [15] R. De Farias Campos, E. Couto, J. De Oliveira, and A. Nied, "On-Line Parameter Identification of an Induction Motor With Closed-Loop Speed Control Using the Least Square Method," *Journal of Dynamic Systems, Measurement, and Control*, vol. 139, no. 7, 071010, 2017.
- [16] R. Bighamian, H. R. Mirdamadi, and J. O. Hahn, "Damage Identification in Collocated Structural Systems Using Structural Markov Parameters," *Journal of Dynamic Systems, Measurement, and Control*, vol. 137, no. 4, 041001, 2015.
- [17] M. D. L. Dalla Vedova and P. C. Berri, "Interactions Problems in Hydraulic Systems: Proposal of a New Nonlinear Speed Control Law Method," *International Journal of Mechanics and Control*, vol. 18, no. 1, pp. 39-44, 2017.
- [18] I. Palomba, D. Richiedei, and A. Trevisani, "Kinematic State Estimation for Rigid-Link Multibody Systems by means of Nonlinear Constraint Equations," *Multibody System Dynamics*, vol. 40, no. 1, pp. 1-22, 2017.
- [19] I. Palomba, D. Richiedei, and A. Trevisani, "Two-Stage Approach to State and Force Estimation in Rigid-Link Multibody Systems," *Multibody System Dynamics*, vol. 39, no. 1-2, pp. 115-134, 2017.
- [20] T. Sands, "Nonlinear-Adaptive Mathematical System Identification," *Computation*, vol. 5, no. 4, 47, 2017.

- [21] M. Cooper, P. Heidlauf, and T. Sands, "Controlling Chaos - Forced Van Der Pol Equation," *Mathematics*, vol. 5, no. 4, 70, 2017.
- [22] F. L. Lewis, D. Vrabie, and V. L. Syrmos, *Optimal Control*, John Wiley and Sons, 2012.
- [23] H. K. Khalil, *Nonlinear Control*, Prentice Hall, New Jersey, 2014.
- [24] C. Hermosilla, R. Vinter, and H. Zidani, "HamiltonJacobiBellman Equations for Optimal Control Processes with Convex State Constraints," *Systems and Control Letters*, vol. 109, pp. 30-36, 2017.
- [25] F. Y. Wang, H. Zhang, and D. Liu, "Adaptive Dynamic Programming: An Introduction," *IEEE computational intelligence magazine*, vol. 4, no. 2, pp. 39-47, 2009.
- [26] D. V. Rao and N. K. Sinha, "A Sliding Mode Controller for Aircraft Simulated Entry into Spin," *Aerospace Science and Technology*, vol. 28, no. 1, pp. 154-163, 2013.
- [27] X. Lu, Z. Liu, J. Zhang, H. Wang, Y. Song, and F. Duan, "Prior-Information-Based Finite-Frequency H-Infinity Control for Active Double Pantograph in High-Speed Railway," *IEEE Transactions on Vehicular Technology*, vol. 66, no. 10, 7922629, pp. 8723-8733, 2017.
- [28] D. Tomas, J. A. Lozano-Galant, G. Ramos, and J. Turmo, "Structural System Identification of Thin Web Bridges by Observability Techniques Considering Shear Deformation," *Thin-Walled Structures*, vol. 123, pp. 282-293, 2018.
- [29] J. N. Juang and M. Q. Phan, *Identification and Control of Mechanical Systems*, Cambridge University Press, 2001.
- [30] T. Katayama, *Subspace Methods for System Identification*, Springer Science and Business Media, 2006.
- [31] M. Sharifzadeh, A. Farnam, A. Senatore, F. Timpone, and A. Akbari, "Delay-Dependent Criteria for Robust Dynamic Stability Control of Articulated Vehicles," in *International Conference on Robotics in Alpe-Adria Danube Region, Springer, Cham*, pp. 424-432, 2017.
- [32] M. Sharifzadeh, F. Timpone, A. Farnam, A. Senatore, and A. Akbari, "Tyre-road adherence conditions estimation for intelligent vehicle safety applications," in *Advances in Italian Mechanism Science, Springer, Cham*, pp. 389-398, 2017.
- [33] G. Mercere, I. Markovsky, and J. A. Ramos, "Innovation-based Subspace Identification in Open-and Closed-loop," in *IEEE 55th Conference on Decision and Control (CDC)*, pp. 2951-2956, 2016.
- [34] M. D. L. Dalla Vedova, P. Maggiore, L. Pace, and S. Romeo, "Proposal of a Model Based Fault Identification Neural Technique for More-Electric Aircraft Flight Control EM Actuators," *WSEAS Transactions On Systems*, vol. 15, pp. 19-27, 2016.
- [35] A. Alenany, G. Mercere, and J. A. Ramos, "Subspace Identification of 2-D CRSD Roesser Models With Deterministic-Stochastic Inputs: A State Computation Approach," *IEEE Transactions on Control Systems Technology*, vol. 25, no. 3, pp. 1108-1115, 2017.
- [36] J. A. Ramos and G. Mercere, "Subspace Algorithms for Identifying Separable-in-denominator 2D Systems with Deterministic-stochastic Inputs," *International Journal of Control*, vol. 89, no. 12, pp. 2584-2610, 2016.
- [37] A. Ruggiero, M. C. De Simone, D. Russo, and D. Guida, "Sound pressure measurement of orchestral instruments in the concert hall of a public school," *International Journal of Circuits, Systems and Signal Processing*, vol. 10, pp. 75-812, 2016.
- [38] E. Ikonen and K. Najim, *Advanced Process Identification and Control*, CRC Press, 2001.
- [39] T. Liu and F. Gao, *Industrial Process Identification and Control Design: Step-test and Relay-experiment-based Methods*, Springer Science and Business, 2011.
- [40] R. F. Stengel, *Optimal Control and Estimation*, Courier Corporation, 2012.
- [41] S. M. Da Conceicao, C. H. Vasques, G. L. C. M. De Abreu, J. V. Lopes, and M. J. Brennan, "Experimental Identification and Control of a Cantilever Beam Using ERA/OKID with a LQR Controller," *Journal of Control, Automation and Electrical Systems*, vol. 25, no. 2, pp. 161-173, 2014.
- [42] M. C. De Simone, S. Russo, Z. B. Rivera, and D. Guida, "Multibody Model of a UAV in Presence of Wind Fields," in *ICCAIRO 2017 - International Conference on Control, Artificial Intelligence, Robotics and Optimization*, Prague, Czech Republic, 20-22 May, 2017.
- [43] A. Concilio, M. C. De Simone, Z. B. Rivera, and D. Guida, "A New Semi-Active Suspension System for Racing Vehicles," *FME Transactions*, vol. 45, no. 4, pp. 578-584, 2017.
- [44] A. Quatrano, M. C. De Simone, Z. B. Rivera, and D. Guida, "Development and Implementation of a Control System for a Retrofitted CNC Machine by using Arduino," *FME Transactions*, vol. 45, no. 4, pp. 565-571, 2017.
- [45] S. Strano and M. Terzo, "Actuator Dynamics Compensation for Real-time Hybrid Simulation: An Adaptive Approach by means of a Nonlinear Estimator," *Nonlinear Dynamics*, vol. 85, no. 4, pp. 2353-2368, 2016.
- [46] S. Strano and M. Terzo, "Accurate State Estimation for a Hydraulic Actuator via a SDRE Nonlinear Filter," *Mechanical Systems and Signal Processing*, vol. 75, pp. 576-588, 2016.
- [47] R. Russo, S. Strano, and M. Terzo, "Enhancement of Vehicle Dynamics via an Innovative Magnetorheological Fluid Limited Slip Differential," *Mechanical Systems and Signal Processing*, vol. 70, pp. 1193-1208, 2016.
- [48] S. Strano and M. Terzo, "A SDRE-based Tracking Control for a Hydraulic Actuation System," *Mechanical Systems and Signal Processing*, vol. 60, pp. 715-726, 2015.
- [49] S. Strano and M. Terzo, "A Multipurpose Seismic Test Rig Control via a Sliding Mode Approach," *Structural Control and Health Monitoring*, vol. 21, no. 8, pp. 1193-1207, 2014.
- [50] S. Pagano, R. Russo, S. Strano, and M. Terzo, "Non-linear Modelling and Optimal Control of a Hydraulically Actuated Seismic Isolator Test Rig," *Mechanical Systems and Signal Processing*, vol. 35, no. 1, pp. 255-278, 2013.
- [51] A. Ruggiero, S. Affatato, M. Merola, and M. C. De Simone, "FEM Analysis of Metal on UHMWPE Total Hip Prosthesis During Normal Walking Cycle," in *Proceedings of the XXIII Conference of The Italian Association of Theoretical and Applied Mechanics (AIMETA 2017)*, Salerno, Italy, 4-7 September, 2017.
- [52] M. C. De Simone and D. Guida, "On the Development of a Low Cost Device for Retrofitting Tracked Vehicles for Autonomous Navigation," in *Proceedings of the XXIII Conference of The Italian Association of Theoretical and Applied Mechanics (AIMETA 2017)*, Salerno, Italy, 4-7 September, 2017.
- [53] M. C. De Simone, Z. B. Rivera, D. Guida, "Finite Element Analysis on Squeal-noise in Railway Applications," *FME Transactions*, vol. 46, no. 1, pp. 93-100, 2017.
- [54] T. Lauss, S. Oberpeilsteiner, W. Steiner, and K. Nachbagauer, "The discrete adjoint method for parameter identification in multibody system dynamics," *Multibody System Dynamics*, vol. 42, no. 4, pp. 397-410, 2017.
- [55] C. M. Pappalardo, Z. Zhang, and A. A. Shabana, "Use of Independent Volume Parameters in the Development of New Large Displacement ANCF Triangular Plate/Shell Elements," *Nonlinear Dynamics*, vol. 91, no. 4, pp. 2171-2202, 2018.
- [56] Z. Tian, S. Li, Y. Wang, and B. Gu, "Priority Scheduling of Networked Control System Based on Fuzzy Controller with Self-tuning Scale Factor," *IAENG International Journal of Computer Science*, vol. 44, no. 3, pp. 308-315, 2017.
- [57] S. El Kafhali, and M. Hanini, "Stochastic Modeling and Analysis of Feedback Control on the QoS VoIP Traffic in a single cell IEEE 802.16 e Networks," *IAENG International Journal of Computer Science*, vol. 44, no. 1, pp. 19-28, 2017.
- [58] T. Taniguchi and M. Sugeno, "Trajectory Tracking Controls for Non-holonomic Systems Using Dynamic Feedback Linearization Based on Piecewise Multi-Linear Models," *IAENG International Journal of Applied Mathematics*, vol. 47, no. 3, pp. 339-351, 2017.
- [59] X. Zhang and D. Yuan, "A Niche Ant Colony Algorithm for Parameter Identification of Space Fractional Order Diffusion Equation," *IAENG International Journal of Applied Mathematics*, vol. 47, no. 2, pp. 197-208, 2017.
- [60] C. M. Pappalardo, "A Natural Absolute Coordinate Formulation for the Kinematic and Dynamic Analysis of Rigid Multibody Systems," *Nonlinear Dynamics*, vol. 81, no. 4, pp. 1841-1869, 2015.
- [61] C. M. Pappalardo, M. Wallin, and A. A. Shabana, "A New ANCF/CRBF Fully Parametrized Plate Finite Element," *ASME Journal of Computational and Nonlinear Dynamics*, vol. 12, no. 3, pp. 1-13, 2017.
- [62] C. M. Pappalardo, Z. Yu, X. Zhang, and A. A. Shabana, "Rational ANCF Thin Plate Finite Element," *ASME Journal of Computational and Nonlinear Dynamics*, vol. 11, no. 5, pp. 1-15, 2016.
- [63] D. Guida, F. Nilvetti, and C. M. Pappalardo, "Parameter Identification of a Two Degrees of Freedom Mechanical System," *International Journal of Mechanics*, vol. 3, no. 2, pp. 23-30, 2009.
- [64] C. M. Pappalardo and D. Guida, "On the Lagrange Multipliers of the Intrinsic Constraint Equations of Rigid Multibody Mechanical Systems," *Archive of Applied Mechanics*, vol. 88, no. 3, pp. 419-451, 2018.
- [65] D. Guida and C. M. Pappalardo, "Sommerfeld and Mass Parameter Identification of Lubricated Journal Bearing," *WSEAS Transactions on Applied and Theoretical Mechanics*, vol. 4, no. 4, pp. 205-214, 2009.
- [66] C. M. Pappalardo and D. Guida, "On the use of Two-dimensional Euler Parameters for the Dynamic Simulation of Planar Rigid Multibody Systems," *Archive of Applied Mechanics*, vol. 87, no. 10, pp. 1647-1665, 2017.
- [67] M. A. Jami'in and E. Julianto, "Hierarchical Algorithms of Quasi-Linear ARX Neural Networks for Identification of Nonlinear Systems," *Engineering Letters*, vol. 25, no. 3, pp. 321-328, 2017.

- [68] J. Zhang, L. Yu, and L. Ding, "Velocity Feedback Control of Swing Phase for 2-DoF Robotic Leg Driven by Electro-hydraulic Servo System," *Engineering Letters*, vol. 24, no. 4, pp. 378-383, 2016.
- [69] Q. W. Guo, W. D. Song, M. Gao, and D. Fang, "Advanced Guidance Law Design for Trajectory-Corrected Rockets with Canards under Single Channel Control," *Engineering Letters*, vol. 24, no. 4, pp. 469-477, 2016.
- [70] H. Liu and Y. Li, "Safety Evaluation of a Long-Span Steel Trestle with an Extended Service Term Age in a Coastal Port Based on Identification of Modal Parameters," *Engineering Letters*, vol. 24, no. 1, pp. 84-92, 2016.
- [71] I. I. Lazaro, A. Alvarez, and J. Anzures, "The Identification Problem Applied to Periodic Systems Using Hartley Series," *Engineering Letters*, vol. 21, no. 1, pp. 36-43, 2013.
- [72] Pappalardo, C. M., and Guida, D., 2018, "System Identification Algorithm for computing the Modal Parameters of Linear Mechanical Systems", *Machines*, 6(2), 12.
- [73] C. M. Pappalardo, M. D. Patel, B. Tinsley, and A. A. Shabana, "Contact Force Control in Multibody Pantograph/Catenary Systems," *Proceedings of the Institution of Mechanical Engineers, Part K: Journal of Multibody Dynamics*, vol. 230, no. 4, pp. 307-328, 2016.
- [74] D. Guida and C. M. Pappalardo, "Control Design of an Active Suspension System for a Quarter-Car Model with Hysteresis," *Journal of Vibration Engineering and Technologies*, vol. 3, no. 3, pp. 277-299, 2015.
- [75] C. M. Pappalardo, T. Wang, and A. A. Shabana, "Development of ANCF Tetrahedral Finite Elements for the Nonlinear Dynamics of Flexible Structures," *Nonlinear Dynamics*, vol. 89, no. 4, pp. 2905-2932, 2017.
- [76] D. Guida, F. Nilvetti, and C. M. Pappalardo, "Instability Induced by Dry Friction," *International Journal of Mechanics*, vol. 3, no. 3, pp. 44-51, 2009.
- [77] C. M. Pappalardo, T. Wang, and A. A. Shabana, "On the Formulation of the Planar ANCF Triangular Finite Elements," *Nonlinear Dynamics*, vol. 89, no. 2, pp. 1019-1045, 2017.
- [78] D. Guida, F. Nilvetti, and C. M. Pappalardo, "Dry Friction Influence on Cart Pendulum Dynamics," *International Journal of Mechanics*, vol. 3, no. 2, pp. 31-38, 2009.
- [79] C. M. Pappalardo and D. Guida, "Use of the Adjoint Method for Controlling the Mechanical Vibrations of Nonlinear Systems," *Machines*, vol. 6, no. 2, 19, 2018.
- [80] C. M. Pappalardo and D. Guida, "On the Computational Methods for solving the Differential-Algebraic Equations of Motion of Multibody Systems," *Machines*, vol. 6, no. 2, 20, 2018.
- [81] C. M. Pappalardo and D. Guida, "System Identification and Experimental Modal Analysis of a Frame Structure," *Engineering Letters*, vol. 26, no. 1, pp. 56-68, 2018.
- [82] M. C. De Simone and D. Guida, "Dry Friction Influence on Structure Dynamics," in *COMPADYN 2015 - 5th ECCOMAS Thematic Conference on Computational Methods in Structural Dynamics and Earthquake Engineering*, pp. 4483-4491, 2015.
- [83] D. Guida and C. M. Pappalardo, "A New Control Algorithm for Active Suspension Systems Featuring Hysteresis," *FME Transactions*, vol. 41, no. 4, pp. 285-290, 2013.
- [84] D. Guida and C. M. Pappalardo, "Forward and Inverse Dynamics of Nonholonomic Mechanical Systems," *Meccanica*, vol. 49, no. 7, pp. 1547-1559, 2014.
- [85] C. M. Pappalardo and D. Guida, "Control of Nonlinear Vibrations using the Adjoint Method," *Meccanica*, vol. 52, no. 11-12, pp. 2503-2526, 2017.
- [86] C. M. Pappalardo and D. Guida, "Adjoint-based Optimization Procedure for Active Vibration Control of Nonlinear Mechanical Systems," *ASME Journal of Dynamic Systems, Measurement, and Control*, vol. 139, no. 8, 081010, 2017.
- [87] M. C. De Simone, Z. B. Rivera, and D. Guida, "Obstacle Avoidance System for Unmanned Ground Vehicles by using Ultrasonic Sensors," *Machines*, vol. 6, no. 2, 18, 2018.
- [88] C. M. Pappalardo, "Modelling Rigid Multibody Systems using Natural Absolute Coordinates," *Journal of Mechanical Engineering and Industrial Design*, vol. 3, no. 1, pp. 24-38, 2014.
- [89] M. C. De Simone and D. Guida, "Modal Coupling in Presence of Dry Friction," *Machines*, vol. 6, no. 1, 8, 2018.
- [90] M. C. De Simone and D. Guida, "Identification and control of a Unmanned Ground Vehicle by using Arduino," *UPB Scientific Bulletin, Series D: Mechanical Engineering*, vol. 80, no. 1, pp. 141-154, 2018.